Natural Convection on Both Sides of a Vertical Wall Separating Fluids at Different Temperatures

R. Anderson
A. Bejan
Assoc. Mem. ASME

Department of Mechanical Engineering,
University of Colorado,
Boulder, Colo. 80309

This paper describes an analytical study of laminar natural convection on both sides of a vertical conducting wall of finite height separating two semi-infinite fluid reservoirs of different temperatures. The countercurrent boundary layer flow formed on the two sides is illustrated via representative streamlines, temperature and heat flux distributions. The net heat transfer between reservoirs is reported for the general case in which the wall thermal resistance is not negligible relative to the overall reservoir-to-reservoir thermal resistance.

Introduction

The engineering importance of heat transfer by natural convection is widely recognized. For example, in the area of energy conservation in buildings natural convection is often responsible for prohibitively large heat leaks to the environment. This and many other applications have stimulated a strong interest in the phenomenon, reflected in an impressive volume of research at the fundamental and applied level.

A central natural convection geometry in many applications is the transfer of heat across a vertical wall separating two semi-infinite fluid reservoirs at different temperatures (see Fig. 1). This problem is of fundamental importance for a variety of reasons. From the insulation engineering point of view, it is important to know the net heat transfer rate across solid walls and windows separating a warm room from a colder environment. From the point of view of fundamental research in heat transfer and fluid mechanics, it is important to understand the interaction of two convective systems coupled across a partially conducting wall.

In spite of the importance of coupled flows, the existing work on natural convection is centered on the study of surfaces with specified heat flux or temperature distributions. We are familiar with only a few examples which allow the heat flux and temperature distribution to be determined by the interaction between adjacent boundary layers [1, 2]. Recently, the first author developed an approximate solution based on the hypothesis that the wall heat flux is uniform [3]. This analysis is outlined in the Appendix. The only other attempt to analyze the configuration shown in Fig. 1 appears to be due to Lock and Ko who reported a numerical solution for heat transfer valid in the limit where the solid wall thermal resistance is negligible [4].

Our objective in this paper is to present an analytical solution for the problem of two countercurrent free convective flow fields separated by a vertical plate with a wide range of conductive resistance. The great advantage of an analytical approach is that the parametric dependence of the heat transfer mechanism is considerably more visible than in a numerical solution. To our knowledge, the present report contains the only analysis and results applicable to situations in which the solid wall thermal resistance is not negligible relative to the two boundary layer resistances formed on either side of the wall.

Mathematical Formulation

In dimensionless form, the equations expressing conservation of mass, momentum and energy for each boundary layer shown in Fig. 1 are

$$\frac{\partial u}{\partial x}+\frac{\partial v}{\partial y}=0 \tag{1}$$

$$\frac{1}{\mathrm{Pr}}\frac{\partial}{\partial y}\left(u\frac{\partial u}{\partial x}+v\frac{\partial u}{\partial y}\right)=\frac{\partial t}{\partial y}+\frac{\partial^3 u}{\partial y^3} \tag{2}$$

$$u\frac{\partial t}{\partial x}+v\frac{\partial t}{\partial y}=\frac{\partial^2 t}{\partial y^2} \tag{3}$$

$$x=\frac{X}{H} \tag{4}$$

$$y=Y/\ell \tag{5}$$

$$t=[T-(T_H+T_C)/2]/(T_H-T_C) \tag{6}$$

The height of the wall, H, is used as length scale in the vertical direction. The horizontal length scale of the boundary layers is ℓ, while T_H and T_C are the dimensional temperatures of the hot and cold fluids. It can be shown via dimensional analysis that [5]

$$\ell=[\nu\alpha H/\beta g\Delta T]^{1/4} \tag{7}$$

while the vertical velocity scale is $\alpha H/\ell^2$

In writing equations (1–3) the terms involving viscous dissipation and gravity work have been ignored. It was assumed that the Boussinesq approximation applies, i.e., that the bouyancy force is proportional to the local temperature difference. The dependence of all other physical properties upon temperature was neglected.

The appropriate boundary conditions in the horizontal (y) direction are

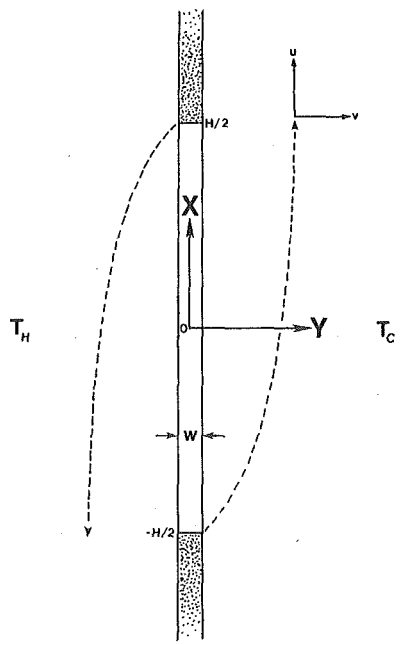

Fig. 1 Schematic of vertical conducting wall with natural convection boundary layers on either side

Contributed by the Heat Transfer Division for publication in the JOURNAL OF HEAT TRANSFER. Manuscript received by the Heat Transfer Division December 3, 1979.

$$u = v = 0 \text{ at } y = \pm w/2 \tag{8}$$

$$t = \mp 1/2 \text{ at } y = \pm \infty \tag{9}$$

In addition, at any given vertical position (x) the heat flux entering the left face of the plate must equal the flux leaving the right face,

$$\left(\frac{\partial t}{\partial y}\right)_{y=-w/2,x} = \left(\frac{\partial t}{\partial y}\right)_{y=w/2,x} = \frac{k_w}{k_f}\left(\frac{\partial t}{\partial y}\right)_{\text{wall}} \tag{10}$$

An important observation is that the governing equations and boundary conditions (1–10) remain unchanged after simultaneously changing the sign of u,v,x,y and t. Therefore, the temperature and velocity fields are centro-symmetric with respect to the origin of the x–y coordinate system shown in Fig. 1,

$$u(x,y) = -u(-x,-y), \tag{11}$$

$$v(x,y) = -v(-x,-y) \tag{12}$$

$$t(x,y) = -t(-x,-y). \tag{13}$$

Equations (1–3) are difficult to treat analytically due to the nonlinearity in the convection part of the energy equation. One way to circumvent this difficulty is to linearize the energy equation according to the modified Oseen technique developed by Gill [5]. In a recent note Bejan [6] showed that Gill's technique produces excellent overall heat transfer results. Linearization is accomplished by regarding v and $\partial t/\partial x$ in equation (3) as unknown functions of altitude, $\bar{v}(x)$ and $\bar{t}'(x)$.

Consider the limit $\text{Pr} \to \infty$, in which the boundary layer equations become

$$\partial u/\partial x + \partial v/\partial y = 0 \tag{14}$$

$$\partial t/\partial y + \partial^3 u/\partial y^3 = 0 \tag{15}$$

$$(\bar{t}')u + (\bar{v})\frac{\partial t}{\partial y} = \frac{\partial^2 t}{\partial y^2} \tag{16}$$

As shown in the Appendix and Fig. 8, the $\text{Pr} \to \infty$ approximation is acceptable in the case of fluids with Prandtl number of order one or greater. Eliminating t between equations (15) and (16) leads to a fourth order ordinary differential equation in $u(x,y)$. The solution to this equation has the general form

$$u = \sum_{n=1}^{4} A_n(x) e^{\lambda_n(x)y} \tag{17}$$

where λ_n are the roots of the characteristic equation

$$\lambda^3(\lambda - \bar{v}) + \bar{t}' = 0 \tag{18}$$

Applying the boundary conditions and symmetry properties, equations (8–13), we obtain

$$u_C = \frac{-(t_0 - Q + 1/2)}{(\lambda_1^2 - \lambda_2^2)}\left(e^{\lambda_1(y-w/2)} - e^{\lambda_2(y-w/2)}\right) \tag{19}$$

$$t_C = \frac{(t_0 - Q + 1/2)}{(\lambda_1^2 - \lambda_2^2)}\left(\lambda_1^2 e^{\lambda_1(y-w/2)} - \lambda_2^2 e^{\lambda_2(y-w/2)}\right) - 1/2 \tag{20}$$

$$u_H = \frac{-(t_0 + Q - 1/2)}{(\xi_1^2 - \xi_2^2)}\left(e^{-\xi_1(y+w/2)} - e^{-\xi_2(y+w/2)}\right) \tag{21}$$

$$t_H = \frac{(t_0 + Q - 1/2)}{(\xi_1^2 - \xi_2^2)}\left(\xi_1^2 e^{-\xi_1(y+w/2)} - \xi_2^2 e^{-\xi_2(y+w/2)}\right) + 1/2 \tag{22}$$

In the above equations $t_0(x)$ is an unknown function representing the temperature distribution along the midplane $y = 0$. For reasons discussed in detail by Gill [5], $\lambda_{1,2}$ are the roots with negative real parts. In addition

$$\xi_{1,2} = -\lambda_{1,2}(-x) \tag{23}$$

and

$$Q = \left|\frac{w}{2}\left(\frac{\partial t}{\partial y}\right)_{\text{wall}}\right|. \tag{24}$$

Since $\lambda_{1,2}$ and $\xi_{1,2}$ are all solutions of equation (18) we can write

$$(\lambda - \lambda_1)(\lambda - \lambda_2)(\lambda + \xi_1)(\lambda + \xi_2) = 0 \tag{25}$$

Expanding result (25) and comparing it with equation (18) we obtain

$$\bar{v}(x) = \lambda_1 + \lambda_2 - (\xi_1 + \xi_2) \tag{26}$$

$$\bar{t}'(x) = (\lambda_1\lambda_2)(\xi_1\xi_2) \tag{27}$$

$$\xi_1\xi_2 + \lambda_1\lambda_2 = (\lambda_1 + \lambda_2)(\xi_1 + \xi_2) \tag{28}$$

$$(\lambda_1\lambda_2)(\xi_1 + \xi_2) = (\xi_1\xi_2)(\lambda_1 + \lambda_2) \tag{29}$$

The solution is simplified if we define two new functions of x, p(even) and q(odd),

$$p = \lambda_1 + \lambda_2 + \xi_1 + \xi_2 \tag{30}$$

$$q = \frac{\bar{v}}{p} \tag{31}$$

Combining these definitions with equations (26–29) allows expressions for $\lambda_{1,2}$ and $\xi_{1,2}$ in terms of the unknown functions $p(x)$ and $q(x)$

$$\lambda_1 + \lambda_2 = 1/2\, p(1 + q) \tag{32}$$

$$\xi_1 + \xi_2 = 1/2\, p(1 - q) \tag{33}$$

$$\lambda_1\lambda_2 = 1/8\, p^2(1 - q^2)(1 + q) \tag{34}$$

$$\xi_1\xi_2 = 1/8\, p^2(1 - q^2)(1 - q) \tag{35}$$

$$\lambda_{1,2} = 1/4\, p(1 + q)[1 \pm i\sqrt{1 - 2q}] \tag{36}$$

$$\xi_{1,2} = 1/4\, p\,(1 - q)[1 \pm i\sqrt{2q + 1}] \tag{37}$$

Functions p and q can be determined from the heat flux continuity constraint, equation (10), and the condition that the linearized solution (19–22) must satisfy the energy equation in intergral form

$$\frac{d}{dx}\left(\int_0^\infty u t dy\right) + |vt|_0^\infty = \left|\frac{\partial t}{\partial y}\right|_0^\infty \tag{38}$$

As parameter w approaches zero, the vertical wall becomes a thin membrane whose face-to-face temperature difference is negligible compared with the overall ΔT between the fluid reservoirs. Substituting $w = 0$ into equations (19–22) and utilizing the heat flux constraint (10) we find

$$\frac{(1/2 - t_0)[(\xi_1 + \xi_2)^2 - \xi_1\xi_2]}{(\xi_1 + \xi_2)} = \frac{(1/2 + t_0)[(\lambda_1 + \lambda_2)^2 - \lambda_1\lambda_2]}{(\lambda_1 + \lambda_2)} \tag{39}$$

Nomenclature

Bi_x = wall local Biot number, $h_x W/k_w$
g = gravitational acceleration
Gr = Grashof number, Ra/Pr
H = wall (window) height
K = constant of integration
ℓ = horizontal length scale, equation (7)
Nu = Nusselt number, hH/k_f
p = even function of x, equation (30)
Pr = Prandtl number
q = odd function of x, equation (31)
Q = wall temperature drop, equation (24), $\text{Bi}_x/2$
Ra = Rayleigh number, $g\beta H^3\Delta T/(\alpha\nu)$
T = temperature
u = vertical velocity
v = horizontal velocity
W = wall thickness
X = vertical position
Y = horizontal position
α = thermal diffusivity
β = coefficient of thermal expansion
ν = kinematic viscosity
ψ = streamfunction
ω = wall parameter, equation (53)

Subscripts

C = ambient conditions on the cold (right) side of the plate
f = fluid
H = ambient conditions on the hot (left) side of the plate
w = wall
0 = conditions at midplane of plate
∞ = ambient conditions on either side of plate

The integral energy constraint (38) applied to each side of the membrane yields

$$\frac{d}{dx}\left[\frac{(t_1 + 1/2)^2}{(\lambda_1 + \lambda_2)^3}\right] = \frac{2(t_0 + 1/2)(\lambda_1^3 - \lambda_2^3)}{(\lambda_1^2 - \lambda_2^2)} \tag{40}$$

$$\frac{d}{dx}\left[\frac{(t_0 - 1/2)^2}{(\xi_1 + \xi_2)^3}\right] = \frac{2(t_0 - 1/2)(\xi_1^3 - \xi_2^3)}{(\xi_1^2 - \xi_2^2)} \tag{41}$$

In terms of p and q, equation (39) can be written as

$$t_0 = -q/(1 + q^2). \tag{42}$$

Finally, writing equations (40) and (41) in terms of p and q, adding side by side and integrating the result once yields

$$p = [(1 - q)^7 + (1 + q)^7]^{1/3}/[K(1 - q^2)(1 + q^2)^{2/3}] \tag{43}$$

Parameter K appearing in equation (43) is an arbitrary constant of integration. Substitution of equation (43) into equation (40) produces a first order ordinary differential equation for the unknown function $x(q)$,

$$\frac{dx}{dq} = [-112\,K^4(1 + q^2)^{5/3}(1 - q^2)^5]/[(1 - q)^7 + (1 + q)^7]^{7/3}. \tag{44}$$

The boundary conditions necessary for solving (44) are based on the approximation that the vertical velocity and horizontal temperature gradient are zero at the beginning of the two boundary layers.

$$u = 0 \text{ at } 0 \le y \le \infty,\ x = -1/2 \tag{45}$$

$$u = 0 \text{ at } -\infty \le y \le 0,\ x = +1/2 \tag{46}$$

$$\frac{\partial t}{\partial y} = 0 \text{ at } y = 0,\ x = \pm 1/2 \tag{47}$$

Condition (45) can be satisfied if $t_0 = -1/2$ or, $\lambda_{1,2} \to \infty$ when $x = -1/2$. This is equivalent to setting $q = 1$ in expression (42).

$$q = +1,\ t_0 = -1/2 \text{ at } x = -1/2 \tag{48}$$

Applying similar arguments to the descending boundary layer in the hot fluid leads to the result

$$q = -1,\ t_0 = 1/2 \text{ at } x = 1/2 \tag{49}$$

Since t_0 is an odd function of q in (42) it is also an odd function of x, hence

$$t_0 = 0,\ q = 0 \text{ at } x = 0. \tag{50}$$

Wall with Finite Thickness

A procedure similar to that used for the thin membrane was also applied to the more general case of finite w. Substitution of equations (19–22) into equation (10) yields

$$t_0 = -q(1 - 2Q)/(1 + q^2) \tag{51}$$

$$Q = -\omega p(1 - q^2)^2/[16(1 + q^2) - 2\omega p(1 - q^2)^2] \tag{52}$$

$$\omega = \frac{W}{H}\frac{k_f}{k_w}\,\mathrm{Ra}^{1/4}. \tag{53}$$

As shown in the Nomenclature, $2Q$ is the wall local Biot number, Bi_x. When the energy integral (38) is applied to the cold side one finds

$$\frac{d}{dx}\{(t_0 - Q + 1/2)^2/[p^3(1 + q)^3]\} = -Q/2\omega. \tag{54}$$

Adding this result to the corresponding energy integral for the hot side and integrating once produces

$$\frac{(1 - q)^7 + (1 + q)^7}{[4(1 + q^2) - \frac{\omega}{2}p(1 - q^2)^2]^2 p^3(1 - q^2)^3} = \frac{K^3}{16} \tag{55}$$

where K is a constant of integration. The value of this constant was determined by integrating equation (54) numerically, trying different values for K until conditions (48–50) were satisfied. The resulting function $K(\omega)$ is listed in Table 1. An important value in this table is $K(0) = -0.6362$ which corresponds to the thin wall limit; this value can also be obtained by integrating equation (44) subject to conditions (48–50).

Results

Figures 2(*a*,*b*) illustrate a set of representative streamlines and isotherms obtained in the thin wall limit ($\omega = 0$). The streamfunction ψ was defined in the usual way by writing $u = \partial\psi/\partial y$ and $v = -\partial\psi/\partial x$. As in Fig. 1, the warm reservoir is on the left side of the picture. The streamlines reveal a descending boundary layer on the warm side coupled with a centrosymmetric ascending boundary layer on the cold side. In the vicinity of the solid wall ($y = 0$) the isotherms are nearly parallel, particularly in the central region. This feature implies that the heat flux is nearly constant along the wall, as shown by the curve $\omega = 0$ in Fig. 6. The slight tilt of the isotherms indicates that the boundary layers transfer heat from the upper left to the lower right across the thin wall.

The wall temperature distribution resulting from the coupled flows is summarized in Figs. 3 and 4. In Fig. 3 we plotted the temperature distribution in the mid-plane ($y = 0$) of the vertical wall, for a series

Table 1 Constant K and overall heat transfer rate $\mathrm{Nu/Ra}^{1/4}$ as a function of ω

ω	K	$\lvert\mathrm{Nu/Ra}^{1/4}\rvert$
0	−0.6362	0.2575
0.2	−0.6232	0.2422
0.4	−0.6113	0.2285
0.6	−0.6004	0.2164
0.8	−0.5903	0.2057
1.0	−0.5809	0.1961
2.0	−0.5422	0.1594
4.0	−0.4891	0.1170
6.0	−0.4529	0.0929
8.0	−0.4259	0.0773
10.0	−0.4047	0.0663
20.0	−0.3390	0.0389

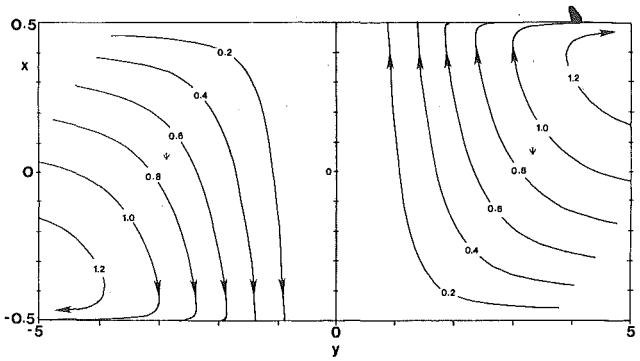

Fig. 2(*a*) Streamline pattern

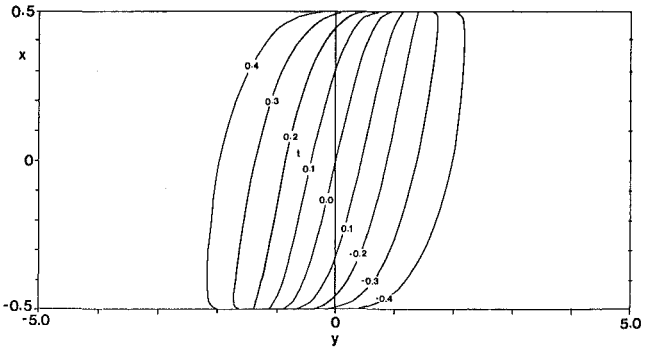

Fig. 2(*b*) Temperature field, in the thin wall limit ($\omega = 0$)

Fig. 2

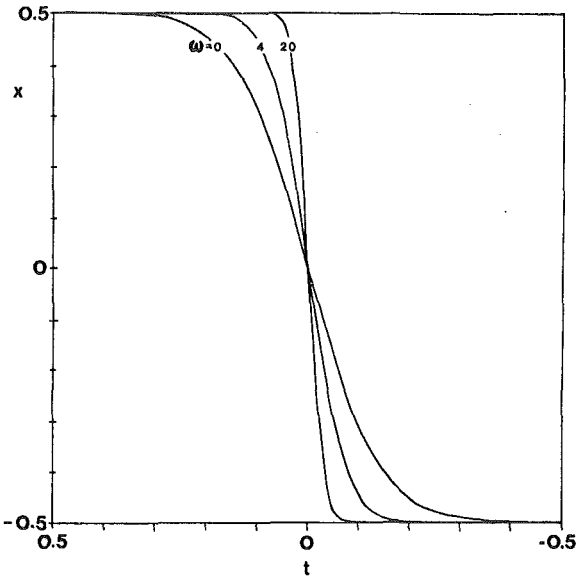

Fig. 3 Temperature distribution in mid-plane ($y = 0$)

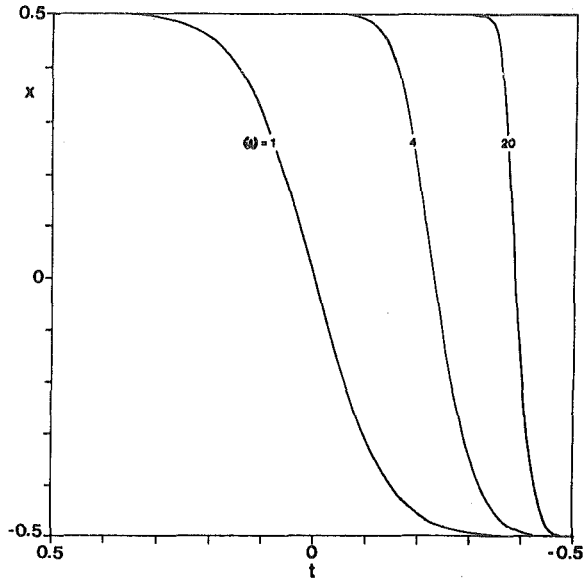

Fig. 4 Temperature distribution over the solid surface facing the cold reservoir

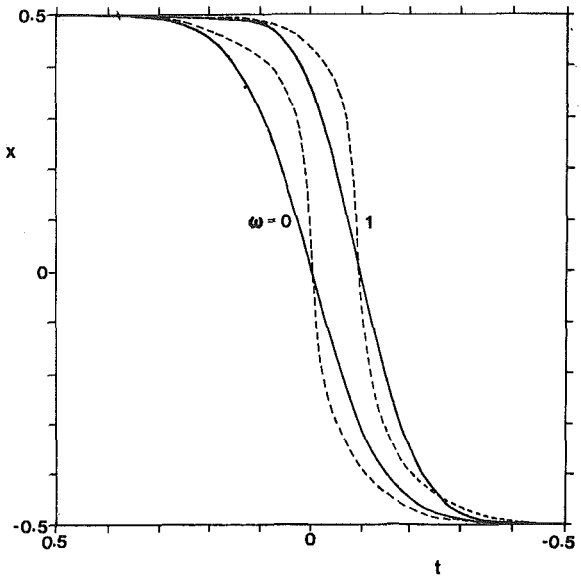

Fig. 5 Comparison of the present result (——) for surface temperature against the numerical solution of Lock and Ko (- - -)

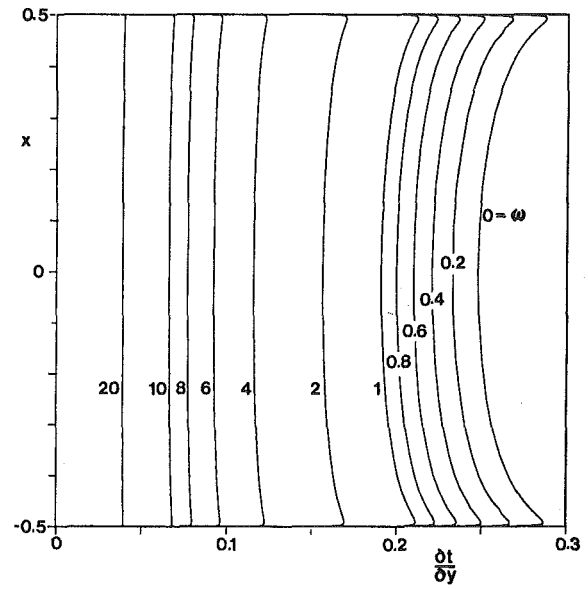

Fig. 6 The distribution of heat flux along the vertical wall

of values of thickness parameter ω. The mid-plane temperature becomes more and more uniform as the wall thermal resistance increases, i.e., as the thermal contact between the two boundary layers deteriorates. Figure 4 shows the corresponding temperature distribution on the surface facing the cold reservoir; the results for the surface facing the warm reservoir are readily obtained by rotating Fig. 4 by 180 deg. It is clear that as the wall becomes thicker the surface-to-surface temperature difference increases to the point where, for $\omega = 20$, it is roughly 80 percent of the reservoir-to-reservoir temperature difference.

In their numerical study of the same phenomenon, Lock and Ko [4] graphed results for Pr = 0.72 and a limited range of wall thickness, ω. In Fig. 5 we compare our results for cold side surface temperature with the results of Lock and Ko, for $\omega = 0$ and $\omega = 1$. The two solutions agree in an average sense, although the numerical solution [4] describes a relatively more uniform surface temperature in the central region of the plate. The constant flux solution developed in the Appendix predicts that the surface temperature distribution will become more nearly isothermal as Pr $\rightarrow$ 0. Hence, the discrepancy between the two sets of curves on Fig. 5 is attributed to the different Prandtl numbers used in each investigation.

The wall heat flux is presented in Fig. 6 as the horizontal temperature gradient $(\partial t/\partial y)_{y=w/2}$. The heat flux decreases as the thickness parameter ω increases. This effect is to be expected since a thicker wall means more effective insulation between the two reservoirs.

Regardless of ω, the wall heat flux is nearly uniform over most of the height H. This observation is the basis for the constant heat flux analysis [3] summarized in the Appendix. In this analysis the wall heat flux is assumed independent of vertical position x and the natural convection problem of Fig. 1 is reconstructed by piecing together two Sparrow and Gregg [7] solutions for convection along a vertical constant heat flux surface, via pure conduction through a wall of finite thickness. The cold surface temperature distribution predicted by the constant heat flux analysis is presented in Fig. 7 vis-a-vis results based on the analysis developed in this paper. The agreement is excellent expecially as ω increases, which is the limit where the constant heat flux assumption is more appropriate.

Overall Heat Transfer

Defining the heat transfer coefficient in terms of the average heat flux through the wall and the total temperature difference between fluid reservoirs

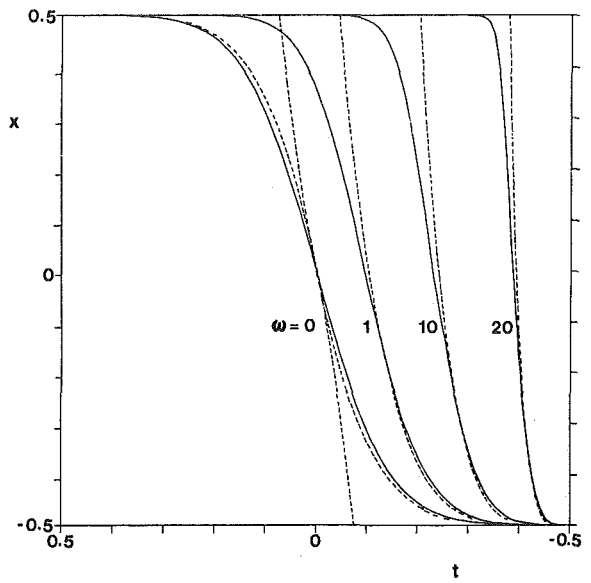

Fig. 7 Comparison of the present result for cold surface temperature (——) against the result based on the constant heat flux approximation (- - -)

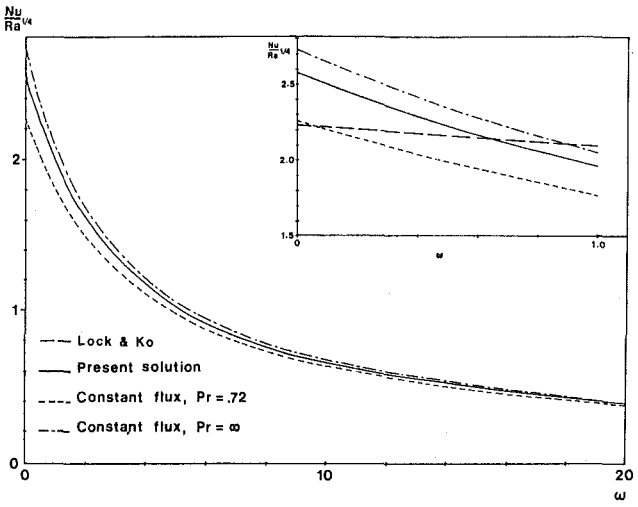

Fig. 8 Dependence of total heat transfer rate on wall resistance parameter ω

$$h = \bar{q}/\Delta T = \frac{k_f}{\Delta T}\left(\frac{\partial \bar{T}}{\partial Y}\right)_{y=w/2} = \frac{k_f}{\ell}\left(\frac{\partial \bar{t}}{\partial y}\right)_{y=w/2} \tag{56}$$

the Nusselt number can be written as

$$\mathrm{Nu} = \frac{Hh}{k_f} = \frac{H}{\ell}\left(\frac{\partial \bar{t}}{\partial y}\right)_{y=w/2} = \mathrm{Ra}^{1/4}\left(\frac{\partial \bar{t}}{\partial y}\right)_{y=w/2}. \tag{57}$$

Figure 8 shows the Nusselt number predicted by our solution and the estimate based upon the constant flux approximation for Pr = 0.72 and Pr → ∞. The agreement between the two solutions is excellent over the entire ω range of interest. The ratio $\mathrm{Nu}/\mathrm{Ra}^{1/4}$ decreases substantially as the wall thickness increases from 0 to 10. Recalling that the present solution was obtained in the limit Pr → ∞ and that the constant heat flux result is Pr dependent, Fig. 8 demonstrates that the overall heat transfer rate is a weak function of Pr provided Pr is of order one or greater. Representative values for $\mathrm{Nu}/\mathrm{Ra}^{1/4}$ for the present solution are shown in Table 1.

Overall heat transfer calculations in the range examined by Lock and Ko are presented in the inset of Fig. 8. The numerical result [4] predicts a weaker dependence on wall thickness than either the present solution or the constant heat flux analysis.

Concluding Remarks

In this paper we analyzed the fundamentals of laminar free convective heat transfer across a vertical wall sandwiched between two fluid reservoirs at different temperatures. In order to gain some insight into the fluid mechanics and basic heat transfer mechanism we constructed an analytical solution based on the Oseen linearization approach without making assumptions about the heat flux or temperature distribution at the wall. We were able to illustrate streamlines and isotherms for the flow field. We also presented results for the distribution of temperature and heat flux along the vertical wall. The effect of increasing wall thermal resistance was documented.

The engineering importance of this study is that it reports means for estimating the reservoir-to-reservoir heat transfer for cases in which the thermal resistance of the wall is not negligible. Prior to our study, the heat transfer literature contained information on overall heat transfer only in the limited range $0 < \omega < 1$. Another conclusion of our study is that the vertical wall can be approximated as a constant flux surface and that the overall heat transfer rate is relatively independent of Prandtl number, for Pr of order 1 or larger.

Acknowledgment

This work was supported in part by NSF Grant ENG 78-20957. The authors thank Professors B. Gebhart and J. C. Mollendorf of the State University of New York at Buffalo, for their comments and for pointing out the existence of reference [4].

APPENDIX

Constant Heat Flux Analysis

Sparrow and Gregg [7] report the following wall temperature distribution for a constant flux surface

$$T_w - T_\infty = f(\mathrm{Pr})\left(\frac{q}{k_f}\right)^{4/5} X^{1/5}\left[\frac{g\beta}{\nu^2}\right]^{-1/5} \tag{A1}$$

where T_w and T_∞ are the dimensional temperatures at the wall and at infinity, and X is the distance measured from the start of the boundary layer. The temperature at $X = H/2$ on the surface facing the cold fluid is

$$\frac{T_H + T_C}{2} + \frac{W}{2}\frac{k_f}{k_w}\left(\frac{\partial T}{\partial Y}\right)_{Y=W/2}. \tag{A2}$$

Substituting this for T_w in (A1) and rearranging we find

$$q^{4/5} = \frac{\Delta T}{2}\left(1 + \omega\left(\frac{\partial t}{\partial y}\right)_{y=w/2}\right)(k_f{}^{4/5})\left(\frac{g\beta}{\nu^2}\right)^{1/5} \Big/ [(H/2)^{1/5} f(\mathrm{Pr})] \tag{A3}$$

which, in combination with (A1), yields

$$\frac{T_w - T_\infty}{\Delta T} = \frac{1}{2}\left(1 + \omega\left(\frac{\partial t}{\partial y}\right)_{y=w/2}\right)\left(\frac{X}{H/2}\right)^{1/5} \tag{A4}$$

Defining h as $q/\Delta T$, the Nusselt number is

$$\mathrm{Nu} = \frac{hH}{k_f} = \frac{1}{2[f(\mathrm{Pr})]^{5/4}}\mathrm{Gr}^{1/4}\left(1 + \omega\left(\frac{\partial \bar{t}}{\partial y}\right)_{y=w/2}\right)^{5/4} \tag{A5}$$

Sparrow and Gregg [7] report a solution for $f(\mathrm{Pr})$ derived using the Karman-Pohlhausen method,

$$\left(\frac{1}{f(\mathrm{Pr})}\right)^{5/4} = \frac{2^{5/4}\,\mathrm{Pr}^{1/2}}{(360)^{1/4}\,(0.8 + \mathrm{Pr})^{1/4}} \tag{A6}$$

Substituting now (A6) into (A5) we obtain

$$\mathrm{Nu} = \left[\frac{\mathrm{Pr}}{0.8 + \mathrm{Pr}}\right]^{1/4}\frac{\mathrm{Ra}^{1/4}}{(180)^{1/4}}\left[1 + \omega\left(\frac{\partial \bar{t}}{\partial y}\right)_{y=w/2}\right]^{5/4}. \tag{A7}$$

Since

$$h = \frac{k_f}{\Delta T}\left(\frac{\partial \bar{T}}{\partial Y}\right) = \frac{k_f}{\ell}\left(\frac{\partial \bar{t}}{\partial y}\right)_{y=w/2} \tag{A8}$$

Table A1 $Nu/Ra^{1/4}$ for constant heat flux solution

	$Nu/Ra^{1/4}$	
ω	Pr = 0.72	Pr = ∞
0	0.226	0.273
0.2	0.214	0.256
0.4	0.203	0.241
0.6	0.194	0.227
0.8	0.185	0.215
1.0	0.177	0.205
2.0	0.147	0.165
4.0	0.110	0.120
6.0	0.088	0.095
8.0	0.074	0.079
10.0	0.064	0.067
20.0	0.038	0.039

we can write

$$Nu = Ra^{1/4}\left(\overline{\frac{\partial t}{\partial y}}\right)_{y=w/2}. \tag{A9}$$

Combining (A9) and (A7) results in

$$\left(\overline{\frac{\partial t}{\partial y}}\right)_{y=w/2} = \left(1 + \omega\left(\overline{\frac{\partial t}{\partial y}}\right)_{y=w/2}\right)^{5/4}\left[\frac{Pr}{(0.8 + Pr)(180)}\right]^{1/4} \tag{A10}$$

Equation (A10) was solved numerically to establish the relationship between $\overline{\partial t/\partial y}_{y=w/2}$ and ω. Temperature distributions for the constant flux approximation are shown in Fig. 7 and the variation of $Nu/Ra^{1/4}$ with ω is shown in Fig. 8. Values for $(\overline{\partial t/\partial y})$ are shown in Table A1. Note that $|\partial t/\partial y|$ decreases with Pr. Equation (A4) implies a wall temperature distribution which is more isothermal in the central region of the plate for small values of Pr.

References

1 Kelleher, M. D., and Yang, K. T., "A Steady Conjugate Heat Transfer Problem with Conduction and Free Convection," *Applied Science Research*, Vol. 17, 1967, pp. 249–269.

2 Lock, G. S. H., and Gunn, J. C., "Laminar Free Convection from a Downward-Projecting Fin," ASME JOURNAL OF HEAT TRANSFER, Vol. 90, No. 1, Feb. 1968, pp. 63–70.

3 Anderson, R., "Heat Transfer through a Thin Membrane Bounded by Fluids with Different Temperatures," term paper, course M.E. 563, (M. C. Branch and D. R. Kassoy, instructors) University of Colorado, May 16, 1979.

4 Lock, G. S. H., and Ko, R. S., "Coupling through a Wall between Two Free Convective Systems," *International Journal of Heat and Mass Transfer*, Vol. 16, 1973, pp. 2087–2096.

5 Gill, A. E., "The Boundary-Layer Regime for Convection in a Rectangular Cavity," *Journal of Fluid Mechanics*, Vol. 26, 1966, pp. 515–536.

6 Bejan, A., "Note on Gill's Solution for Free Convection in a Vertical Enclosure," *Journal of Fluid Mechanics*, Vol. 90, 1979, pp. 561–568.

7 Sparrow, E. M., and Gregg, J. L., "Laminar Free Convection for a Vertical Surface with Uniform Surface Heat Flux, *Trans ASME*, Vol. 78, 1956, pp. 435–440.